DIELECTRIC BREAKDOWN WEATHERING: MORPHOLOGICAL EFFECTS OF ELECTRICAL BREAKDOWN IN LABORATORY-IRRADIATED SAN CARLOS OLIVINE. M. L. Shusterman[1], T. G. Sharp[1], and M. S. Robinson[1]. [1]School of Earth and Space Exploration, Arizona State University, Tempe, AZ. (morgan.shusterman@asu.edu).

Introduction: The conventional perspective on space weathering is that optical maturation of regolith is a function of micrometeoroid bombardment, solar wind irradiation, and gardening. However, theoretical models [1-4] indicate dielectric breakdown may ubiquitously and significantly affect optical signatures of airless bodies at rates similar to those of micrometeoroid bombardment [5,6]. Evidence of dielectric breakdown weathering may have been detected in the lunar maria [6], yet no corroborating evidence has been identified in the Apollo sample collection. Few laboratory experiments have investigated the potential contribution of dielectric breakdown to overall weathering [7,8].

The dielectric strength of a material defines the maximum electric field tolerated prior to failure of the material's insulating properties. That failure, dielectric breakdown, results in the formation of plasma channels that rapidly propagate to facilitate charge dissipation. The high-pressure, high-temperature expansion of these channels within solids results in permanent physical and chemical alterations including fracturing, vaporization, and melting [9]. On the Moon and other airless bodies, sufficient potential to overcome the dielectric strength of regolith is supplied during solar energetic particle (SEPs) events [1].

Here, we present results of a laboratory-irradiated San Carlos olivine. The purpose of this investigation was to compare morphologies between physical damage caused by dielectric breakdown and reported lunar sample patinas. This study focused on alterations made to the sample surface, but we will report on alterations generated at depth at a later date.

Experimental Methodology: Two sections of a non-oriented, gem-quality San Carlos olivine were cut to 3x3x1.5 mm and hand polished with alumina suspensions to minimize surface defects.

Using methods similar to [8], the sections were placed under vacuum (~10^{-6} torr) and a 30 kV focused electron beam was continuously rastered, with a flux of ~$1.9x10^{15}$ electrons cm^{-2} s^{-1}, over uncoated regions measuring ~90 µm x 100 µm. Because discharge timescales are anticorrelated to material temperature, we used a large flux to overcome the charge dissipation rate of olivine at room temperature. The total scan time was modulated between two and twenty minutes across eight experimental runs, delivering estimated fluences of 10^{17}-10^{18} electrons cm^{-2}.

Each section was carbon coated after irradiation and imaged with an FEI XL-30 scanning electron microscope.

Results: In seven of the eight experimental runs, we identified physical signatures of dielectric breakdown including discharge pathways, melt deposition, and pits created by plasma channels erupting to the surface.

A dense network of dendritic channels and melt deposits, including droplets with diameters 40-300 nm, formed within each of the seven regions (Fig. 1a). Experiments with lower total fluence yielded a lower areal density of breakdown channels and melt deposits. In all cases, the areal density of breakdown features abruptly decreased at the scan boundary. These results are consistent with [8].

While the majority of damage was contained within each scan region, some discharge pathways extended up to 30 µm outside the scan boundary. Near these smaller channels it is possible to better understand the quantity and areal distribution of melt produced by only a few breakdown events (Fig. 1b).

Once breakdown channels have been formed, they act as preferential pathways for subsequent discharges. While surface scratches were not found to influence discharge pathways, several pre-existing fractures were exposed to the surface as discharges propagated along these features (white arrow in Fig. 1c).

In addition to surface discharges, there was evidence of eruptive plasma channels originating at depth and consistent with deep dielectric charging (Fig. 1d). Diameters of these pits ranged from 70-750 nm, with the majority of the population having a diameter of 100-400 nm. Pits wider than 100 nm commonly had prominent splash melt deposits.

Discussion: The alterations produced by dielectric breakdown in olivine are consistent with small craters, accretionary glass spherules, and etched surfaces defined by [10] as "classic patina" on Apollo 17 sample 76015. The vaporization of material also generates amorphous rims, another classic characteristic of space weathered minerals. However, isotopic analysis is required to determine the similarity between rims formed by dielectric breakdown in the lab and those formed by exposure to the space environment.

Dendritic channels similar to those we observed have not been identified in the Apollo sample collection but this may be the result of using a single olivine crystal. The angularity, granularity, and polycrystalline nature of regolith creates an electrical environment that is

not precisely replicated by charging of a monomineralic single-crystal sample, but we expect that certain types of physical alterations (i.e., vaporization, melting, and fracturing) should be common across most insulating solid materials undergoing dielectric breakdown. The use of high flux may have also contributed to the presence of surficial breakdown channels via non-equilibrium reactions, but ohmic heating was minimal.

Conclusion: Dielectric breakdown weathering is predicted to significantly contribute to the optical maturation of minerals on airless bodies across the solar system. The results of this ongoing study support the idea that dielectric breakdown can produce physical damage that is typically attributed to the effects of solar wind irradiatiom and micrometeoroid impacts.

See abstract #1270 [11] for a discussion about the conditions under which dielectric breakdown may occur and its implications for laboratory-based space weathering studies.

Acknowledgments: We would like to acknowledge the use of facilities within the Eyring Materials Center at Arizona State University.

References: [1] Jordan et al., (2014) *JGR: Planets*, *119*, 1806-1821. [2] Jordan et al., (2015) *JGR: Planets*, *120*, 210-225. [3] Jordan et al., (2018) *Icarus*, *319*, 785-794. [4] Zimmerman et al., (2016) *JGR:Planets*, *121,* 2150-2165. [5] Jordan et al., (2019) Icarus, 283. 352-358. [6] Jordan, A. J. (2021), *Icarus*, *In press*. [7] Campins and Krider (2003) *Science*, *248*, 622-624. [8] Lemelle et al., (2003) *Geochim. Cosmochim. Acta.*, *67*, 1901-1910. [9] Budenstein P. P. (1980) *IEEE*, *EI-15*, 225-240. [10] Wentworth et al., (1999) *Meteor. & Planet Sci., 34*, 593-603. [11] Jordan, A. P. (2021) *LPSC, LII*, #1270.

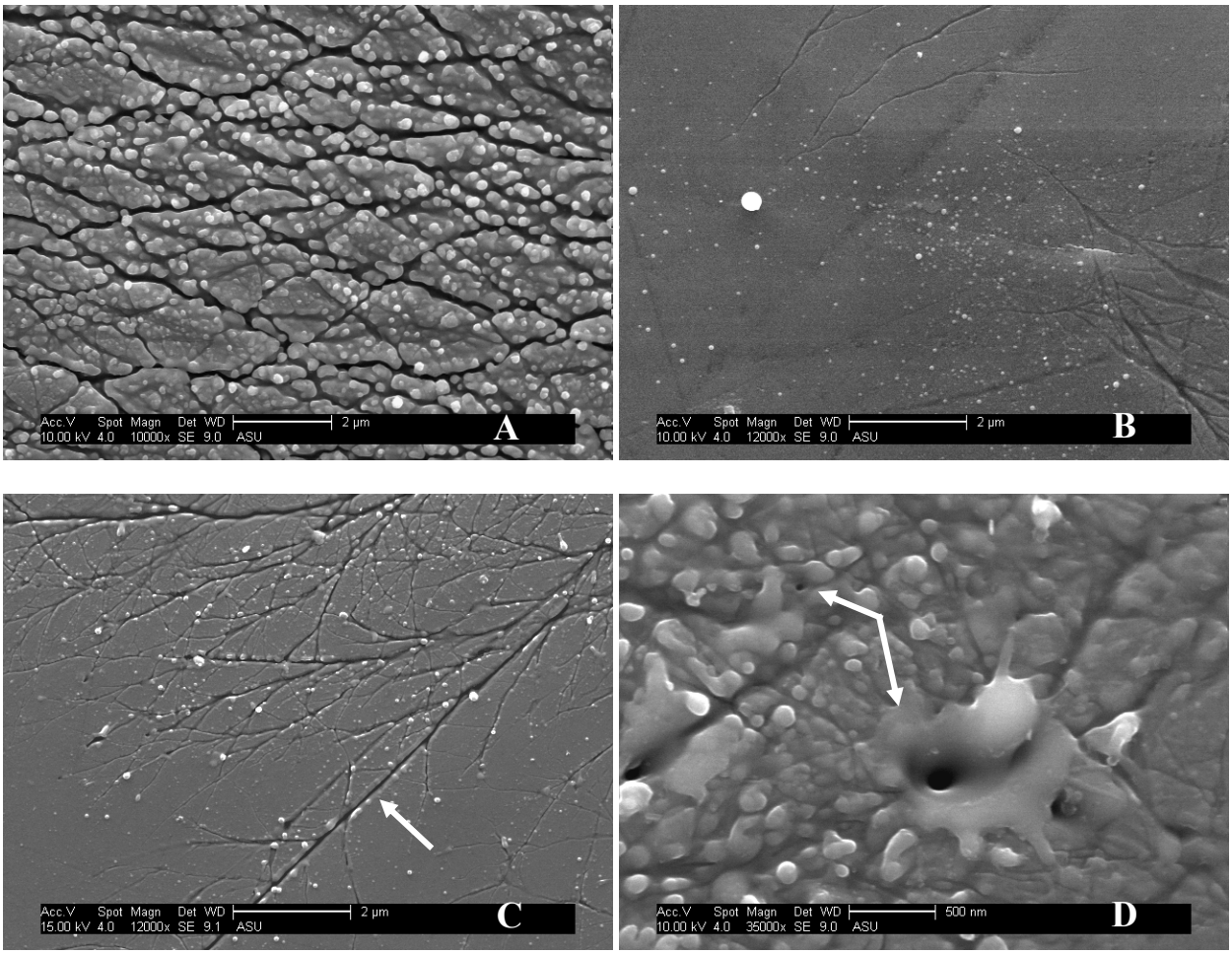

Figure 1. Secondary electron (SEM) images of dielectric breakdown-induced damage in San Carlos olivine. (**a**) Inside the scan boundary, rapid and repeated electrical discharges formed deep breakdown channels and areally dense melt deposits. **(b)** Approximately 20 µm from the scan boundary, ionization channels were significantly shallower than in (a) and melt deposition was much more sparse. **(c)** Pre-existing fractures (white arrow) provided preferential pathways for discharge. **(d)** Eruptive channels were most commonly identified near scan boundaries. While most of these features had melt skirts, this feature was absent in the smallest population.